Journal of Environmental Health Science and Engineering (2019) 17:685–700
https://doi.org/10.1007/s40201-019-00384-9

RESEARCH ARTICLE

Degradation of dimethyl phthalate using persulfate activated by UV and ferrous ions: optimizing operational parameters mechanism and pathway

Mojtaba Yegane Badi[1,2] · Ali Esrafili[1,2] · Hasan Pasalari[1,2] · Roshanak Rezaei Kalantary[1,2] · Ehsan Ahmadi[3,5] · Mitra Gholami[1,2] · Ali Azari[4,3,5]

Received: 12 March 2019 / Accepted: 10 June 2019 / Published online: 12 July 2019

Abstract

The present study aimed to model and optimize the dimethyl phthalate (DMP) degradation from aqueous solution using UV_C/$Na_2S_2O_8$/Fe^{2+} system based on the response surface methodology (RSM). A high removal efficiency (97%) and TOC reduction (64.2%) were obtained under optimum conditions i.e. contact time = 90 min, SPS concentration = 0.601 mM/L, Fe^{2+} = 0.075 mM/L, pH = 11 and DMP concentration = 5 mg/L. Quenching experiments confirmed that sulfate radicals were predominant radical species for DMP degradation. The effect of CO_3^- on DMP degradation was more complicated than other aquatic background anions. The possible pathway for DMP decomposition was proposed according to HPLC and GC–MS analysis. The average oxidation state (AOS) and carbon oxidation state (COS) values as biodegradability indicators demonstrated that the UV_C/SPS/Fe^{2+} system can improve the bioavailability of DMP over the time. Finally, the performance of UV_C/SPS/Fe^{2+} system for DMP treatment in different aquatic solutions: tap water, surface runoff, treated and raw wastewater were found to be 95.7, 88.5, 80.5, and 56.4%, respectively.

Keywords DMP · Sulfate radicals · Statistical analysis · BBD · Degradation pathway

Introduction

Rapid growth of chemicals consumption in industries have produced wastewater with high toxicity and refractory substances, which have caused environmental, economical and health-related issues over the recent years [1, 2]. Phthalate esters (PAE_S), as predominant chemicals in industries, are often incorporated as softening agent. Dimethyl phthalate ester (DMPE) is one of the phthalates widely used for producing polyvenil chloride resin, adhesive material and colour. They are commenly used in home furnishings, aeterial structures, food pockets and polyvinylchloride (PVC) resins [3, 4]. Phthalate esters are classified as recalcitrant, hazardous and emeging contaminants [5–7]. Unitated states environmental protection agency (USEPA) and europian union (EU) classify the phetalat esters as priority pollutants [8–10]. In recent years, the risk of Phthalate compounds which impact endocrine [11], reproduction, and even cause cancers [12] and abortion [10] have drawn much attention. On the other hand, lack of proper wastewater treatments, inappropriate disposal methods of

Electronic supplementary material The online version of this article (https://doi.org/10.1007/s40201-019-00384-9) contains supplementary material, which is available to authorized users.

✉ Mitra Gholami
gholamim@iums.ac.ir; gholamimitra32@gmail.com

✉ Ali Azari
Azari.hjh@gmail.com

[1] Research Center for Environmental Health Technology, Iran University of Medical Sciences, Tehran, Iran

[2] Department of Environmental Health Engineering, School of Public Health, Iran University of Medical Sciences, Tehran, Iran

[3] Department of Environmental Health Engineering, School of Public Health, Tehran University of Medical Sciences, Tehran, Iran

[4] Department of Environmental Health Engineering, School of Public Health, Kashan University of Medical Sciences, Kashan, Iran

[5] Students' Scientific Research Center (SSRC), Tehran University of Medical Sciences, Tehran, Iran

industrial effluent have excaberated issues associated with phetalat esters discharge to the environmnet [13]. Advanced oxidation processes (AOP) coupled with light irradiation are noticeably employed for remediation of water/wastwater pollutants [14, 15]. These processes tend to generate hydroxyl radicals which are highly reactive and nonselective oxidants toward organic compounds [16]. In last decades, SPS have been incorporated as high-performance and strong in chemical oxidation of pollutants [17]. High soulubility in water, high affinity to react with contaminants, and lower production of hazardous by-products are the part of SPS advantages [18, 19]. In the present research, persulfate anion (PS) with a redox potential of 2.01 were selected for following reasons. Firstly, PS as strong oxidant can be induced to produce stronger radicals ($SO_4^{\circ-}$), with more redox potential changing between 2.5 and 3.1 V [20]. Furthermore, the produced $SO_4^{\circ-}$ reacts 10^3–10^5 times faster in comparision with the persulfate under the same conditions [21, 22]. In 2017, Ghaneian et al., conducted a research on 2,4-D removal by AOP basesd sulfate radicals systems and suggested S_2O_8/UV with efficient for removal of this organic pollutant from aquatic solution [23]. Among a variety of available methods, bivalent iron (Fe^{2+}), as a catalyst can dramatically convert SPS to SO°_4. Indeed, presence of Fe^{2+} by improving and increasing the production of sulfate-free radicals can improve contaminant degradation, considerably. The chemical interactions occured between $S_2O_8^{2-}$ and Fe^{2+} are given in (Eq. 1–12) [24, 25].

$$\mathbf{S_2O_8^{2} \xrightarrow{hv} 2SO_4^{\circ-}} \quad \Phi = 1.4\text{–}1.8 \tag{1}$$

$$SO_4^{\cdot-} + SO_4^{\cdot-} \rightarrow S_2O_8^{2-} \quad K = 5.0 \times 10^8 M^{-1}S^{-1} \tag{2}$$

$$SO_4^{\cdot-} + S_2O_8^{2-} \rightarrow SO_4^{2-} + S_2O_8^{\cdot-} K = 1.2 \times 10^6 M^{-1}S^{-1} \tag{3}$$

$$Fe^{2+} + S_2O_8^{2-} \rightarrow Fe^{3+} + SO_4^{2-} + SO_4^{\cdot-} K = 2.7 \times 10^1 M^{-1}S^{-1} \tag{4}$$

$$SO_4^{\cdot-} + Fe^{2+} \rightarrow SO_4^{2-} + Fe^{3+} \quad K = 3.0 \times 10^8 M^{-1}S^{-1} \tag{5}$$

$$SO_4^{\cdot-} + OH^- \rightarrow SO_4^{2-} + HO^{\cdot} K = (6.5 \pm 1.0) \times 10^7 M^{-1}S^{-1} \tag{6}$$

$$SO_4^{\cdot-} + H_2O \rightarrow SO_4^{2-} + HO^{\cdot} + H^+ \quad K < 60\ M^{-1}S^{-1} \tag{7}$$

$$HO^{\cdot} + SO_4^{\cdot-} \rightarrow HSO_5^- K = (0.95 \pm 0.08) \times 10^{10} M^{-1}S^{-1} \tag{8}$$

$$HO^{\cdot} + S_2O_4^{\cdot-} \rightarrow OH^- + S_2O_8^{\cdot-} K < 1.0 \times 10^6 M^{-1}S^{-1} \tag{9}$$

$$Fe^{2+} + HO^{\cdot} \rightarrow Fe^{3+} + OH^- K = 3.2 \times 10^8 M^{-1}S^{-1} \tag{10}$$

$$Fe^{3+} + hv \rightarrow Fe^{2+} + HO^{\cdot} \quad \Phi = 0.07 \tag{11}$$

$$Fe^{3+} + HO_2^{\cdot} \rightarrow Fe^{2+} + O_2 + H^+ K < 1.0 \times 10^3 M^{-1}S^{-1} \tag{12}$$

Rao et al. [26] conducted a study on ibuprofen degradation by UV/Fe/PS system and observed that simultaneous application of UV and Fe has a significant role in persulfate activating and facilitate the degradation process. Until this part of the research, the role of UV and Fe in DMP degradation was expressed. One-factor-at-a-time (OFAT) strategy has been employed in many studies to determine the sample sizes and testing procedures, regardless the economic issues and the weakness of this method in examining interaction effect of variables. However, RSM which take advantages of mathemateical and statistical technique have recently drawn much attention by researchers for process development and process optimization. The most advantages imposed on RSM are: minimal numbers of experiments, less consumable chemicals and accordingly less corresponding cost and energy consumption. Box-Behenken design (BBD) is organized to be the most widely utilized optimization technique for the AOPs process due to the benefits of optimizing several factor problems with the ideal number of test runs regarding to response surface methodology (RSM) [27–29]. According to the issues introduced here, this study was therefore developed to (I) examine the efficiency of UV_C/SPS/Fe^{2+} in DMP degradation by considering the effects of operating parameters including pH, contact time, Fe^{2+} and SPS concentration and DMP initial concentration using response surface methodology as statistical approach (II) Predict and optimization the parameters influencing on DMP degradation by RSM-BBD approach (III) examining the role of dominant radicals during the degradation process (IV) Identification the intermediates, by-products and pathway of degradation process using GC-MS and HPLC.

Materials and methods

Chemicals

Methanol (CH_3OH, > 99.8%), iron chloride ($FeCl_2$, ≥99.99%), Sulfuric Acid (H_2SO_4, > 99.8%), sodium hydroxide (NaOH, > 97%), SPS ($Na_2S_2O_8$, ≥99%), Tert-butyl alcohol (t-BuOH, >99%) and Dimethyl phthalate (DMP, >98.7%) with analytical grade were provided from Sigma (Sigma-Aldrich., Germany) and employed as received without further purification. The required solutions throughout the experiments were diluted using Deionized water (DI-water).

Reactor set up and experimental procedure

A tubular reactor made of stainless material and resistant to chemical reaction with a volume of 1 L was applied to perform the experiments. In each run, the aquatic solution along with chemicals used in the experiment were introduced to reactor. The reactor was equipped with two valves at both sides for sampling and chemical solution loading. In addition, the light source consisting a low-pressure Hg lamp (6 W) UV-C lamp (λ = 254 nm), was placed in quartz glass cylinder in the middle of reactor; it provided the UV radiation for reactor. To balance proper mixing and ensure safety, the tubular reactor was placed on leg and shaker with 100 rpm. Sampling was taken at given times according to design of experiments

software, version 10.0.0. Figure 1S shows a schematic of the pilot scale of reactor.

Design of Experiments

Response surface methodology (RSM) is comprised of mathematical and statistical procedures to determine the optimum conditions for experiment by considering the lowest numbers of experiments. To investigate the effects of independent parameters on DMP degradation, the experiments were designed with Box-Benken Design (BBD). The interaction between parameters were analyzed with 3-dimensional (3D) graphs [30]. In the present study, five independent parameters including A (Time, min), B (SPS concentration, mM/L), C (Fe^{2+} concentration, mM/L), D (pH) and E (DMP concentration, mg/L) were considered for analysis. The range of parameters were surveyed in three levels (−1, 0, and + 1). Table 1s shows the range and experimental values of independent parameters. Equation 13 was computed to compare different variables with different units, the actual values of the variables (denoted as Xi) were coded as follows:

$$A_i = \frac{X_i - X_0}{\Delta X} \tag{13}$$

Where, A_i is the coded number of variable, X_i is real value of parameter, Δx is the difference between the high and the median values of the variable and X_0 refers to the median value of the variable. The emperical second-order polynominal model (Eq.14) was employed to explain the behaviour of process.

$$Y = b_0 + \sum_{i=1}^{n} b_i X_i + \sum_{i=1}^{n} b_{ii} X_i^2 + \sum_{i=1}^{n-1} \sum_{j=i+1}^{n} b_{ij} X_i X_j \tag{14}$$

Where, Y is the predicted response, b_0 is a constant while, b_i, bii and bij stand for the linear coefficient, quadratic coefficient and interaction effect coefficient, respectively. X_i and X_j are also the coded values of the variables. Further, analysis of variance (ANOVA) was employed in order to analyeze the results and to figure out the statistical significance of the fitted quadratic models. The optimal values of the critical parameters on DMP degradation under UV_C/SPS/Fe^{2+} system were calculated by using the Desirability Function (DF) approach and then validated based on the results of the experiments. The kinetics of DMP degradation was evaluated in order to investigate the effect of main operational parameters (independent effect) on photocatalytic degradation process through UV_C/SPS/Fe^{2+} system. The first-order reaction (Eq. (15)) was employed to describe the degradation kinetic of DMP in all experiments,

$$\ln\left(\frac{C_t}{C_0}\right) = k_{obs} \times t \tag{15}$$

Where, C_t is the concentration of DMP at any instant time t, and C_0 is the initial concentration of DMP and K_{obs} is the pseudo-first-order rate constant. Based on the linear relationship between ln (C_t/C_0) and time, the assumed first-order kinetics was conformed.

Apparatus and analysis methods

A high-performance liquid chromatography (HPLC, Cecil CE4100) with a UV detector (CE 4900) at 254 nm was utilized to determine the residual concentration levels of DMP throughout the experiments [31]. A discovery C18 column (250 mm × 4.6 mm) was employed to measure residual DMP concentration, and the analyses were carried out with a 65/35 (*v*/v) methanol/water mobile phase at a flow rate of 1.0 mL/min. Gas Chromotography (GC) (Agilent 7890) equipped with Mass Spectrometry Detector (GC-MS) with a column HP-5, length = 25 m, i.d. = 0.12 mm was employed to identify and determine the intermediate and by-products resulting from DMP degredation [32]. After sample injection at 250 °C, the temperatyre program was set as follows: initial oven temperature was adjusted at 50 °C for 3 min and rising to 250 at constant rate of 10 °C min^{-1} and hold for 2 min. The results of the GC–MS analysis were interpreted by comparison with commercial standards in the library records of the National Institute of Standards. Total organic carbon (TOC) was determined by a TOC analyzer (Multi N/C, 3100, Germany). The Electron paramagnetic resonance (EPR) measurements were carried out on Bruker A 300 spectrometer at room temperature (Bruker EMX A300, Ettlingen, Germany).

Results and discussion

DMP removal under various systems

Figure 1 shows the different control experiments in assessment of the activity of single UV irradiation and coupled with $Na_2S_2O_8$ and Fe^{2+} for enhancement of DMP removal. As observed, DMP removal efficiencies for single UV irradiation (50.7%) and SPS (0.51 mM) (7.9%) within 90 min seem not to degrade DMP efficiently. However, application the UV_C/SPS within 90 min significantly increased the DMP removal efficiency (79.2%), representing the formation of reactive oxidizing species. Furthermore, the integration UV_C/SPS/Fe^{2+} process enhanced DMP degradation considerably (92.85%), proving the synergetic effects of the applied agents. This enhancement can be explained by the fact the simultaneous presence of generated OH° and SPS radicals as well as synergistic effect Fe^{2+} as catalysts activate SPS in order to generate more radicals for DMP decomposition [33, 34]. Results obtained from the present study indicated that integration Fe^{2+} with

UV_C and SPS (UV_C/SPS/Fe^{2+}) was as an applicable system for degradation of DMP.

Eeffect of influencing parameters on DMP degradation

pH

The initial pH is an important factor that affect decomposition of target compounds and free radicals produced in the persulfate based advanced oxidation process [35, 36]. The interaction influence of contact time and pH is presented in (Fig. 2S.a). The maximum DMP removal efficiency occurred when pH was maintained at their high level. As shown in (Fig. 2S.**a)**, the highest removal efficiency (86.52%) was observed at pH = 11 and lowest degradation (69.367%) was at pH = 3 (time: 47.5 min, SPS concentration: 0.51 mM, Fe^{2+} concentration: 0.08 mM and DMP concentration: 27.5 mg/L). Improvement the degradation efficiency in alkaline conditions was possibly due to the fact that sulfate radicals can react with hydroxide ions based on eq. 16 and 17 and generate hydroxyl radicals with $E_o = 2.7$ V [37]. The hydroxyl radicals with a high redox potential can lead to increases the degradation efficiency of DMP and their intermediate compounds. In other side, at alkaline pH, in addition to more aggressive oxidation reaction with OH°, oxygen radicals are also produced (see Eq. 18) [38]. Indeed, the simultaneous presence of three radical types including SO_4° and OH° and $O^{\circ-}$ in alkaline conditions make pH = 11 as preferred condition for DMP treatment [39].

$$S_2O_8^{2-} + hv \rightarrow 2SO_4^{\circ-} \quad (16)$$

$$SO_4^{\circ-} + OH^- \rightarrow OH^\circ + SO_4^{2-} \quad (17)$$

$$OH^\circ + OH^- \rightarrow O^{\circ-} + H_2O \quad (18)$$

Moreover, $S_2O_8^{\circ-}$ can be involved in radical chain reactions with water, while freshly generated Fe^{2+} react with $S_2O_8^{2-}$ to generate radical sulfate $SO_4^{\circ-}$ through the following reaction:

$$\equiv Fe^{II} + S_2O_8^{2-} \rightarrow \equiv Fe^{III}OH + SO_4^{2-} + SO_4^{\circ-} \quad (19)$$

Also $SO_4^{\circ-}$ or HO° in reaction SPS can generate the $S_2O_8^{\circ-}$ radicals which improve the degradation performance:

$$SO_4^{\circ-} + S_2O_8^{2-} \rightarrow SO_4^{2-} + S_2O_8^{\circ-} \quad (20)$$

$$HO^\circ + S_2O_8^{2-} \rightarrow HO^- + S_2O_8^{\circ-} \quad (21)$$

Taicheng et.al (2017) investigated the degradation of Dimethyl Phthalate in aqueous solution under UV/persulfate system and found that optimum pH for DMP removal was 10 which is in agreement with the results obtained from the present study [40]. Yegane badi and et.al (2016) reported that the optimum pH for Dimethyl Phthalate (DMP) removal using ultraviolet activated persulfate for oxidation is in alkanine conditions [41].

Reaction time

To survey the influence of the reaction time on UV_C/SPS/Fe^{2+} system, the DMP removal efficiency at 5 different reaction times (5–90 min) was investigated (other conditions were fixed at pH: 11, SPS concentration: 0.51 mM, Fe^{2+} concentration: 0.08 mM and DMP concentration: 27.5 mg/L). According to the Fig. 2S, by increasing the reaction time from 5 to 77 min, the degradation efficiency increased from 77.23 to 89.83%. However, the removal efficiency is augmented with a low slope during 77 to 90 min. As time preceded, oxidation reactions of OH^- continues to lead generation the free radicals including $O^{\circ-}$ and OH° so as to improve the DMP degradation [42, 43]. The DMP degradation process continues to 77 min with proper function, however after that, the efficiency is almost constant. It can be explained by the fact that the intermediate compounds are hypothesized to be resistant in comparison with target contaminant (DMP), which use more free radicals. The results are in agreement with previous reports by Dedong sun (2013), sharma (2015) and Azadbakht (2017) [44, 45].

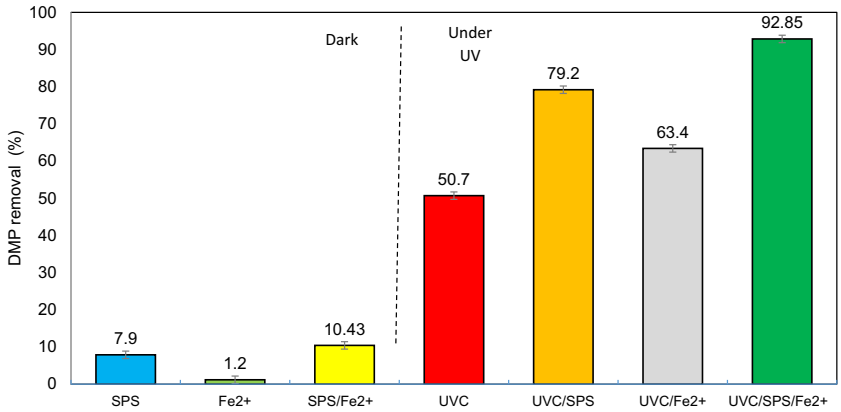

Fig. 1 DMP removal efficiency in different systems over 60 min reaction

SPS concentration

The effect of SPS on DMP degradation under UV_C/SPS/Fe^{2+} system is presented in Fig. 2S.**b**. As shown, the removal efficiency was improved about 12% as SPS concentration increased from 0.21 to 0.6 mM/L, and after that it decreased with gentle slope from 91.38% to 87.05% (experiment conditions pH: 11, reaction time = 77 min, Fe^{2+} concentration: 0.08 mM and DMP concentration: 27.5 mg/L). The decomposition of SPS in aqueous solution is an important step to yield SO_4°, and such SO_4° radicals can also react with H_2O to produce more OH°. The successive reactions of SPS to produce sulfate radicals from $S_2O_8^{2-}$ are presented in (Eq. 22 and 23) [46].

$$S_2O_8^{2-} \rightarrow 2SO_4^{\circ -} \quad (22)$$

$$SO_4^{\circ} + H_2O \rightarrow HO^{\circ} + HSO_4^{-} \quad (23)$$

The generated free radicals can react with the DMP and consequently enhance mineralization rate and removal efficiency. Increases the oxidizing agent concentration (SPS) enhance the reaction rate until a determined level; an inverse trend for DMP degradation was observed at SPS concentration level more than 0.5 mM/L. In concentration > 0.5 mM/L, SPS act as scavenger (free radical quencher) and convert sulfate radicals to SPS or sulfate anion according to the Eqs 24–26. All the reactions discussed earlier make SPS radicals

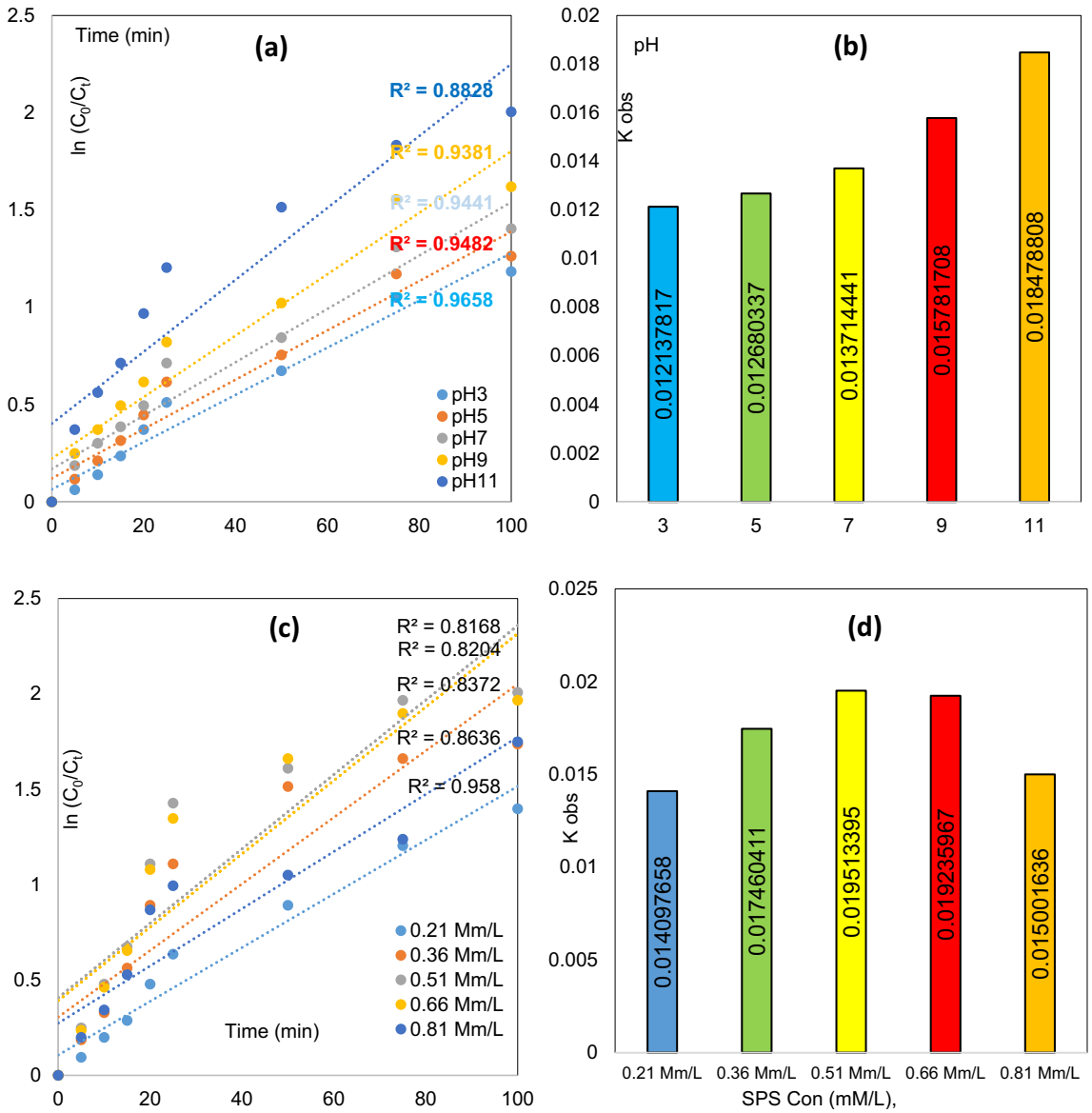

Fig. 2 Kinetic and rate constants of DMP degradation in term of (**a** and **b**) pH, (**c** and **d**) SPS concentration, (e and f) Fe^{2+} concentration and (g and h) DMP concentration under optimum conditions

destroy and lower DMP removal efficiency [47, 48]. The destruction of free radicals and converting them to dissolved ions subsequently result in removal efficiency reduction.

$$SO_4^{\circ-} + OH^{\circ} \rightarrow HSO_4^- + \frac{1}{2}O_2 \quad (24)$$

$$SO_4^{\circ-} + SO_4^{\circ-} \rightarrow 2SO_4^{2-} \text{ or } s_2O_8^{2-} \quad (25)$$

$$SO_4^{\circ-} + S_2O_8^{2-} \rightarrow 2SO_4^{2-} + S_2O_8^{\circ} \quad (26)$$

The results of study conducted by Guo,Y et al. on Tetrabromobisphenol A degradation using microwave/SPS system [49] and Huang, Yi Fong (2009) on BPA degradation by UV/SPS [50] are in line with the present work; increases in SPS concentration more than required level conversely lower the reaction rate and system performance.

Fe^{2+} concentration

Figure 2S.c shows the results of the DMP degradation by SPS activated with ferrous ions at experiment conditions pH: 11, reaction time: 77 min, SPS concentration: 0.5 mM and DMP concentration: 27.5 mg/L. Fe^{2+} can act as efficient activator for converting SPS to sulfate-based free radicals [51]. Indeed, Fe^{2+} ions rapidly activate SPS to sulfate radicals form i.e. $SO4^{\circ-}$. Nevertheless, the high reduction potential of ferrous ions and the high oxidation potential of the $SO4^{\circ-}$ generated could initiate a stronger interaction between Fe^{2+} and $SO4^{\circ-}$. Fe^{2+} ions were converted simultaneously by both SPS and sulfate

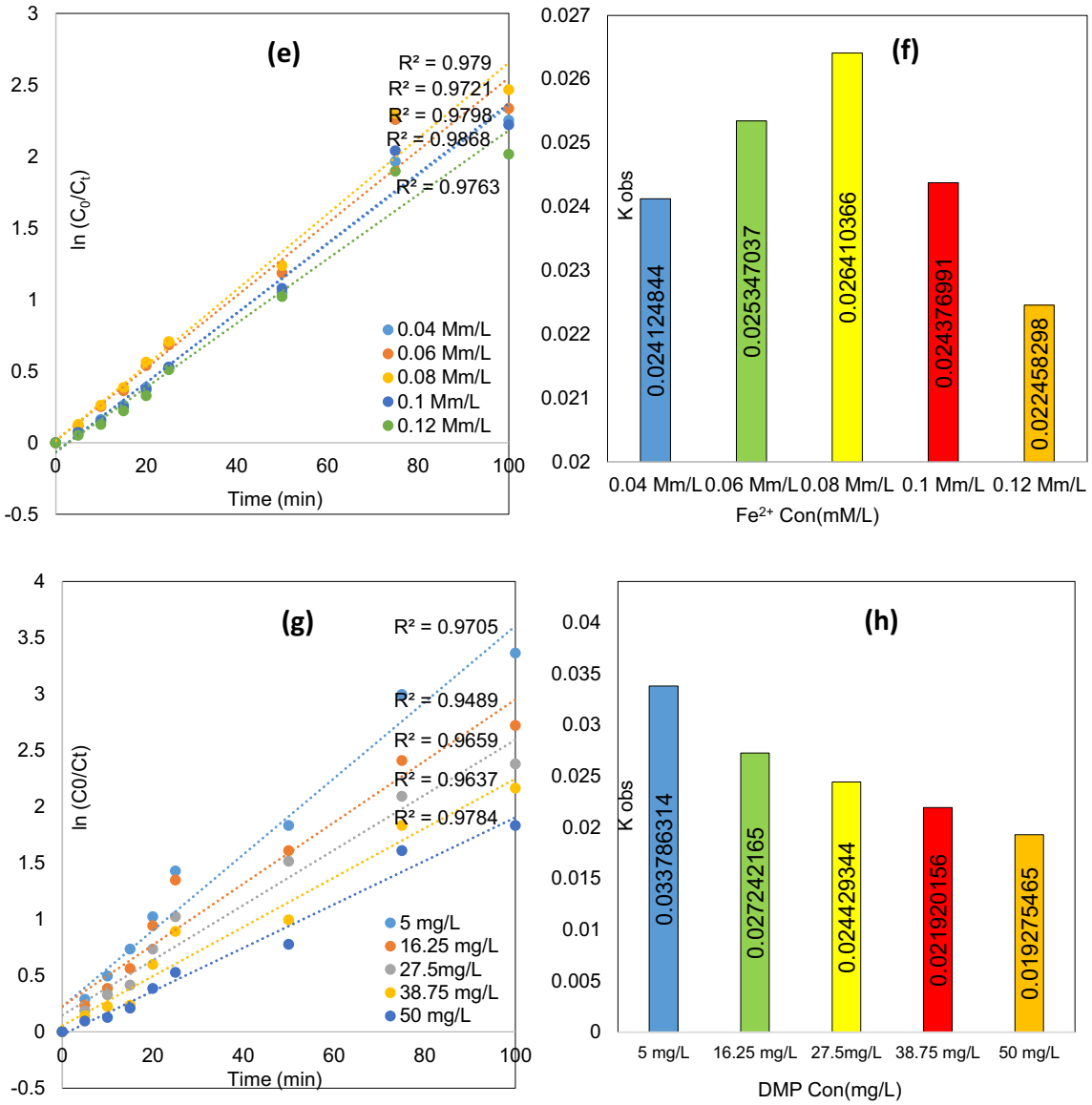

Fig. 2 (continued)

radicals, and the final reaction product (SO_4^{2-}) remained in the system. The reaction equations were as follows [24].

$$S_2O_8^{2-} + 2Fe^{2+} \rightarrow 2Fe^{3+} + SO_4^{\circ-} \quad (27)$$

$$S_2O_8^{2-} + Fe^{2+} \rightarrow Fe^{3+} + SO_4^{2-} + SO_4^{\circ-} \quad (28)$$

$$Fe^{2+} + SO_4^{\circ-} \rightarrow Fe^{3+} + SO_4^{2-} \quad (29)$$

As shown in Eq. 29 sulfate radicals are consumed by ferrous ions. Therefore, we observed that at Fe^{2+} concentration > 0.07 mM/L, the behavior of DMP degradation decreased. In the study conducted by Long Zhao et.al on 1,4-diaxone degradation with $UV_C/SPS/Fe^{2+}$, it was reported that increases in Fe^{2+} until a specific level promotes the removal rate and after that a constant trend is observed, which these results are in agreement with present study [48]. Lin, C.S. and et.al (2012) reported that Fe^{2+} and Cu (II) ions, as intermediate metals, are effective to activate SPS for propachlor degradation in aquatic solutions. The findings of Lin indicated that increases in Fe^{2+} and Cu as catalyst can't improve degradation performance at all conditions, so that higher concentration of mentioned ions cause reduction of removal efficiency [52].

DMP concentration

The influence of initial DMP concentration levels on the performance of $UV_C/SPS/Fe^{2+}$ system was investigated in the range of 5 to 50 mg/L at pH: 11, reaction time = 77 min, SPS concentration: 0.5 mM and Fe^{2+} concentration: 0.07 mM. From Fig. 2S**. d,** it is observed that when DMP concentration levels were increased from 5 to 50 mg/L, the degradation efficiency was reduced from 97.59 to 87.06%. High concentrations of DMP prevents the penetration of UV_C light, and subsequently decrease the interaction between SPS and UV_C light to produce reactive species. On the other hand, fixed values of SPS and Fe^{2+} against high amount of contaminate concentrations is insufficient to completely eliminate DMP which it consequently produces intermediate

Table 1 Results of ANOVA analysis to determine the effect and interaction between factors on DMP degradation

Source	Sum of Squares	df	Mean Square	F-value	p value	
Model	3229.64	20	161.48	2112.26	< 0.0001	significant
A-Time	739.16	1	739.16	9668.54	< 0.0001	
B-SPS Con.	191.13	1	191.13	2500.07	< 0.0001	
C-Fe2+ Con.	2.03	1	2.03	26.56	< 0.0001	
D-pH	1122.25	1	1122.25	14,679.53	< 0.0001	
E-Initial Con.	377.82	1	377.82	4942.01	< 0.0001	
AB	0.0400	1	0.0400	0.5232	0.4762	
AC	0.0025	1	0.0025	0.0327	0.8580	
AD	0.1225	1	0.1225	1.60	0.2172	
AE	0.0306	1	0.0306	0.4006	0.5325	
BC	0.7225	1	0.7225	9.45	0.0050	
BD	0.4225	1	0.4225	5.53	0.0269	
BE	0.2025	1	0.2025	2.65	0.1162	
CD	1.82	1	1.82	23.84	< 0.0001	
CE	0.0400	1	0.0400	0.5232	0.4762	
DE	0.0225	1	0.0225	0.2943	0.5923	
A^2	47.30	1	47.30	618.75	< 0.0001	
B^2	466.01	1	466.01	6095.56	< 0.0001	
C^2	96.43	1	96.43	1261.28	< 0.0001	
D^2	56.80	1	56.80	742.91	< 0.0001	
E^2	10.03	1	10.03	131.16	< 0.0001	
Residual	1.91	25	0.0765			
Lack of Fit	0.9979	20	0.0499	0.2732	0.9837	not significant
Pure Error	0.9133	5	0.1827			
Cor Total	3231.55	45				
Std. Dev.	0.2765		R^2	0.9994		
Mean	72.19		Adjusted R^2	0.9989		
C.V. %	0.3830		Predicted R^2	0.9984		
			Adeq Precision	196.5591		

Table 2 Optimum conditions selected for the maximum possible DMP removal (%) by $UV_C/SPS/Fe^{2+}$ system

Name	Goal	Limit	Limit	Optimum value	Experimental	Predicted	Desirability
Time	In range	5	90	90			
SPS Con.	In range	0.21	0.81	0.601			
Fe^{2+} Con.	In range	0.04	0.12	0.075			
pH	In range	3	11	11			
Initial Con	In range	5	50	5			
Degradation	maximize	55.5	100	97.227	94.35	97.227	0.994

compounds. Therefore, it is hypothesized that the inadequate numbers of free radicals may cause a competition between DMP molecules and the intermediates to react with free radicals. Similar trends have been reported by other researchers for degradation of the DMP by UV/H_2O_2 [53].

Kinetic study

In order to study the kinetic of the process, first order (FO) model was used to fit data obtained from $UV_C/SPS/Fe^{2+}$ oxidation experiments. Therefore, DMP degradation rate under UV_C radiation in the presence of SPS/Fe^{2+} can be expressed as follows:

$$\frac{d(DMP)}{dt} = -K_{DMP}(DMP) \quad (30)$$

Where k_{DMP} is the overall rate constant of the $UV_C/SPS/Fe^{2+}$ process. The simulated FO kinetic at different pH indicated that the k_{DMP} increased from 0.01214 min^{-1} to 0.01847 min^{-1} with increasing pH from 3 to 11 ($R^2 > 0.882$). Above results suggested that the basic condition favor the DMP photo-degradation, which was supported by the fact that OH°, SO_4° and $O^{\circ-}$ simultaneously attempt to decompose DMP pollutant (Fig. 2a, b). The first order rate constant was calculated from 0.01409 min^{-1} to 0.01500 min^{-1} (with goodness of fit $R^2 > 0.82$) at initial SPS concentration from 0.21 mM/L to 0.81 mM/L (Fig. 2c, d). The observed FO kinetic constant of DMP (k_{DMP}) increased from 0.01409 to 0.01951 min^{-1} when the initial SPS concentration was increased from 0.21 to 0.51 mM/L, then slightly decreased to 0.01923 min^{-1} at SPS concentration of 0.66 mM/L and eventually dropped to 0.01500 min^{-1} when the initial SPS was increased to 0.81 mM/L. SPS > 0.51–0.66 mM/L act as scavenger for generated free radicals and inhibited photo-degradation of DMP. Figure 2e, f illustrate the relationship between the k_{DMP} values with various Fe^{2+} concentrations between 0.04 and 0.12 mM/L. Results showed that the k_{DMP} values at Fe^{2+} concentrations of 0.04, 0.06, 0.08, 0.1, and 0.12 mM/L were 0.02412 min^{-1}, 0.02534 min^{-1}, 0.02641 min^{-1}, 0.02437 min^{-1}, and 0.02245 min^{-1}, respectively. Increasing Fe^{2+} concentrations led to the catalyzing the SPS reaction, which produced more $SO4^{\circ-}$ radicals to oxidize DMP and resulted in accelerating the degradation rate. Meanwhile, excessive Fe^{2+} concentration quickly consume SPS or sulfate radical in solution, which can inhibit removal efficiency of DMP. The degradation of DMP through $UV_C/SPS/Fe^{2+}$ system followed FO kinetics with respect to the DMP concentrations with high correlation coefficients ($R^2 \geq 0.949$). As shown in Fig g and h, the k_{DMP} calculated for the studied DMP concentrations were in the order of 0.03378 min^{-1} (5 mg/L) > 0.02724 min^{-1} (16.25 mg/L) > 0.02442 min^{-1} (27.5 mg/L) > 0.02192 min^{-1} (38.75 mg/L)

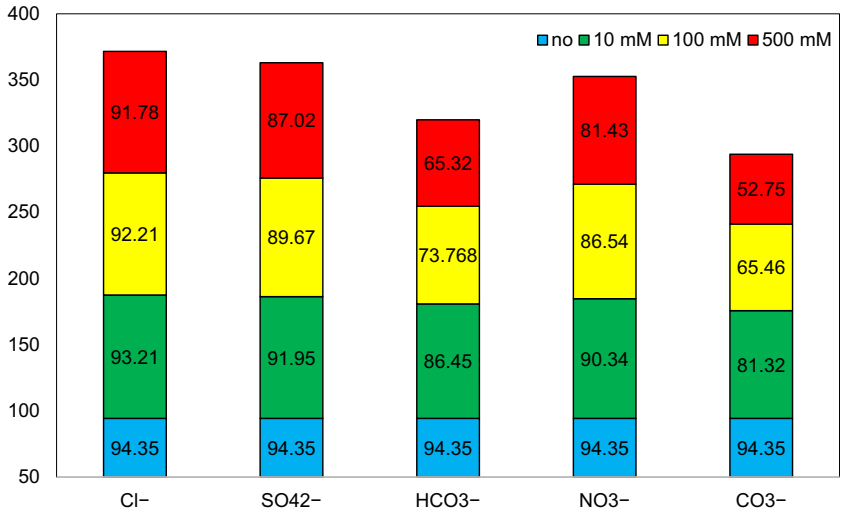

Fig. 3 DMP degradation by $UV_C/SPS/Fe^{2+}$ in term of background materials (dissolved anions in 10, 100 and 500 mM concentrations) under optimized conditions

and > 0.01927 min^{-1} (50 mg/L). The fixed value of generated free radicals versus the high concentrations of DMP cause free radicals not sufficiently destruct DMP molecules and its intermediates. This leads to an inverse relationship between reaction rate and DMP concentration.

Statistical analysis of the parameters

The 5 factors at three levels BBD matrix and the value of the response function (observed and predicted) are presented in Table 1. A total number of 46 experiment runs designed by BBD was analyzed. According to results obtained from the present study, the removal efficiency of the DMP varied between 55.5% and 92.5%. The empirical relationship between independent or influencing experimental variables and removal efficiency (dependent variable) determined by RSM method is shown in Eq. 31:

$$\begin{aligned} \textit{DMP degradation efficiency}\ (\%) = {} & +75.43 + (6.80A) + (3.46B) - (0.36C) + (8.38D) \\ & - \Big(4.E + (0.1AB) + (0.025AC) - (0.18AD) + (0.088AE) + (0.42BC) \\ & + (0.32BD) - (0.23BE) - (0.67CD) - (0.1CE) - (0.075DE) \\ & - \Big(2.33A^2\Big) - \Big(7.31B^2\Big) - \Big(3.32C^2\Big) + \Big(2.55D^2\Big) + (1.07E2) \end{aligned} \tag{31}$$

As denoted in Eq. 33, the factors with negative coefficient have an antagonist effects on response, while positive coefficient indicate a direct relationship between factors and DMP degradation. The highest coefficient belonged to D and lowest related to C, meaning pH and Fe^{2+} concentration have the highest and lowest impact on DMP degradation process, respectively. The results of analysis of variance (ANOVA) were interpreted for individual effect of each factor and interaction between factors on DMP degradation. Statistical variables described in Table 1 reflect that the regression model with p value = 0.0001 and F-Value = 2112.26 is significant and is suitable to spatial modeling. There is just a 0.01% chance that a model F-value this large could happen because of noise. P values fewer than 0.05 reveal that model variables are significant on DMP degradation. In this context, A, B, C, D, E, BC, BD, CD, A^2, B^2, C^2, D^2, E^2 are significant model terms. The Lack of Fit F-value of 0.27 implies the Lack of Fit is not significant relative to the pure error. There is a 98.37% chance that a "Lack of Fit F-value" with this large value could occur due to noise. Lack of fit with non-significant valid that the suggested model can appropriately explain the relationship between response and independent variables [54]. The Predicted R^2 of 0.9984 is in reasonable agreement with the Adjusted R^2 of 0.9989; i.e. the difference is less than 0.2, indicating a good relationship between Predicted-R^2 and Adjusted -R^2 [55]. The "Adequate Precision" measures the signal to noise ratio. A ratio greater than 4 is desirable. Adequate Precision ratio was found to be 196.559 which indicates an adequate signal. Therefore, this model can be utilized to navigate the design space [56].

Adequacy of model

The normal (percentage) probability plot is commonly used to detect and explain the systematic departures. It is assumed that errors are normally distributed, independent of each other and the error variances are homogeneous, as well. A normal probability plot (a dot diagram of these residuals) is shown in supplementary material, Fig. 3S **(a)**. Figure 3S **(b)** shows the relationship between the actual and predicted values of Y for the removal of DMP. As can be seen, the points cluster around the diagonal line indicates a good fit of the model, since the deviation between the experimental and predicted values was less.

Process optimization using the desirability function (DF)

Response surface methodology (RSM) was used to evaluate the optimum conditions for DMP degradation efficiency. In this sense, the DMP removal efficiency with maximum value was defined as response and influencing parameters were considered in their range (See Table 2). The numerically optimal value of each affecting parameter on removal efficiency of DMP are listed in Table 2**.** According to results, the maximum removal efficiency under optimum conditions i.e. contact time = 90 min, SPS concentration = 0.601 mM/L, Fe^{2+} = 0.075 mM/L, pH = 11, and DMP concentration = 5 mg/L was found to be 97.221% (Desirability: 0.97221). To valid the model prediction, a series of additional experiments was performed in triplicate under above-mentioned optimum conditions. The replicated experiments in optimized mode revealed that removal efficiency to be 94.35 ± 2.3. As presented in Table 2, the removal efficiency for response variable in BBD model and laboratory conditions are

in strong agreement, which emphasize the validity and precision of applied model. The findings indicated that RSM is a useful and suitable tool for optimization DMP degradation using $UV_C/SPS/Fe^{2+}$ system.

Effects of background materials on DMP degradation

The aquatic matrix can influence the fate and degradation the target compound. Therefore, the effect of aquatic background materials including Cl^-, SO_4^{2-}, CO_3^{2-}, NO_3^- and HCO_3^- anions on DMP degradation by $UV_C/SPS/Fe^{2+}$ system was investigated under optimum operational conditions. CO_3^{2-} and HCO_3^- inhibited the SPS oxidation of DMP and the inhibiting effects became more pronounced as the CO_3^{2-} and/or HCO_3^- concentration increased. DMP degradation (%) in presence of 10 mM, 100 mM, and 500 mM of CO_3^{2-} and HCO_3^- are presented in Fig. 3. From figure, higher CO_3^{2-} and HCO_3^- resulted in lower DMP degradation efficiencies. According to the Eqs. 32–35, CO_3^{2-} and HCO_3^- can react with $SO_4^{-\circ}$ and OH° to form $CO_3^{\circ-}$ and HCO_3° radicals. As can be seen in the reaction rate constant of the mentioned equations, the transformation of $SO_4^{\circ-}$ and OH° with high oxidation potential to $CO_3^{\circ-}$ and HCO_3° with less reactivity occurred at a relatively fast rate ($\sim 10^6$ M^{-1} s^{-1}); which subsequently leads to reduce the overall oxidation strength of the system [57].

$$SO_4^{\circ-} + CO_3^{2-} \rightarrow SO_4^{2-} + CO_3^{\circ-} \quad K = 6.1 \times 10^6 \ M^{-1} S^{-1} \tag{32}$$

$$SO_4^{\circ-} + HCO_3^- \rightarrow SO_4^{2-} + HCO_3^{\circ-} \quad K = 9.1 \times 10^6 \ M^{-1} S^{-1} \tag{33}$$

$$OH^\circ + CO_3^{2-} \rightarrow OH^- + CO_3^{\circ-} \quad K = 3.91 \times 10^8 \ M^{-1} S^{-1} \tag{34}$$

$$OH^\circ + HCO_3^- \rightarrow H_2O + HCO_3^{\circ-} \quad K = 3.91 \times 10^6 \ M^{-1} S^{-1} \tag{35}$$

The effects of different concentration levels of NO_3^- and SO_4^{2-} on DMP removal efficiency were all very close to the control. NO_3^- can scavenge for $SO_4^{\circ-}$ via Eq. 36 to form NO_3° radical. Nevertheless, this reaction is very slow with reported rate constant of 2.1×10^0 M^{-1} s^{-1} [58]. Hence, the scavenging effect by nitrogen trioxide radical was insignificant, which was possible to be the reason that NO_3^- had no influences on the SPS oxidation of DMP. SO_4^{2-} did not react with $SO_4^{\circ-}$, thus the existence of SO_4^{2-} had no effect on DMP degradation either.

$$SO_4^{\circ-} + NO_3^- \rightarrow SO_4^{2-} + NO_3^\circ \tag{36}$$

The effect of Cl^- on DMP degradation was more complicated than other water matrixes. Cl^- exhibited the reaction with $SO^\circ{}_4^-$ at the rate constant of 3.1×10^8 M^{-1} s^{-1} which could compete for $SO^\circ{}_4^-$ with DPM, and DMP degradation was decreased in the presence of chloride. The high reaction rate constant, indicating that it is very easy for Cl^- to react with $SO_4^{\circ-}$ (based Eq. 37). However, Cl^- could react with $SO_4^{\circ-}$ to produce Cl° which consequently reacts with additional Cl^- to produce $Cl_2^{\circ-}$ (Eq. 38). Compared to $SO_4^{\circ-}$ and Cl°, the $Cl_2^{\circ-}$ have relative lower oxidation potential and less reactivity. Under such conditions, Cl^- acts as a radical scavenger to consume $SO_4^{\circ-}$, which accordingly reduce the overall oxidation strength. Therefore, the presence of Cl^- did not extremely inhibit DMP degradation, and the higher concentration of Cl^- decreased the inhibiting effect of chloride on DMP degradation.

$$SO_4^{\circ-} + Cl^- \rightarrow SO_4^{2-} + Cl^\circ \quad K = 3.1 \times 10^8 M^{-1} S^{-1} \tag{37}$$

$$Cl^\circ + Cl^- \rightarrow Cl_2^{\circ-} \quad K = 8 \times 10^9 \ M^{-1} S^{-1} \tag{38}$$

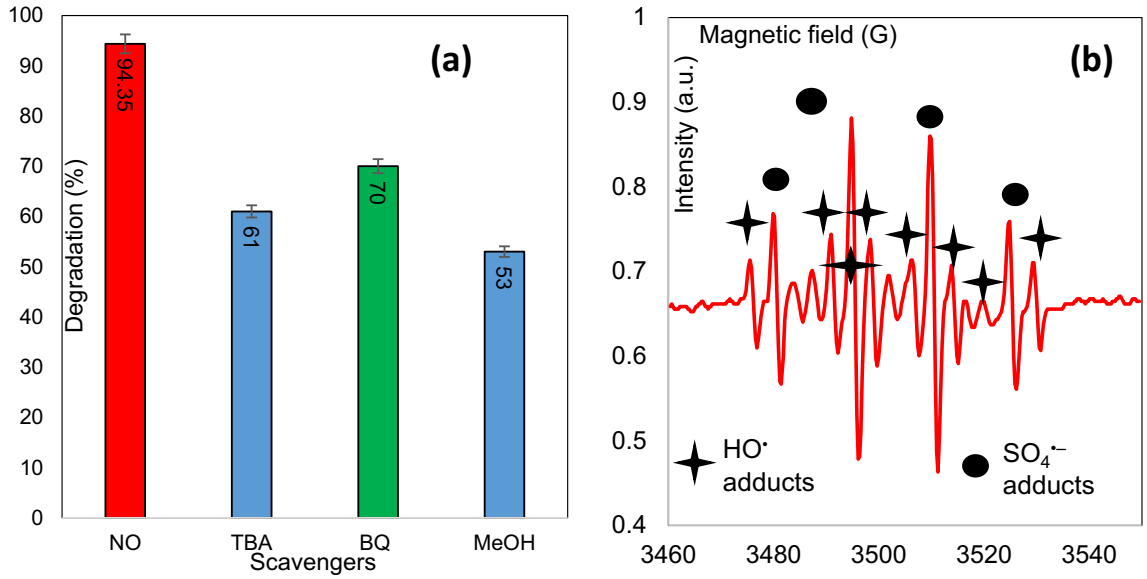

Fig. 4 Photocatalytic degradation of DMP after adding quenching agents (**a**) ESR spectra of radical adducts trapped by superoxide and hydroxyl radical (**b**)

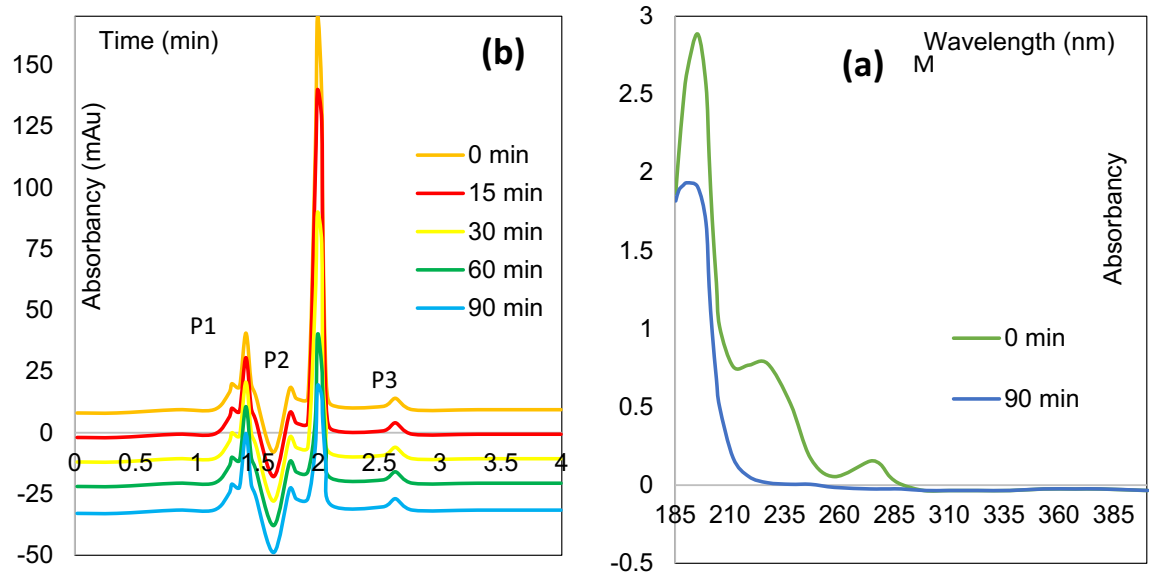

Fig. 5 The variation of UV–vis (**a**) and HPLC (**b**) of DMP solutions during the treatment time of 0 and 90 min

In general, it can be seen that the presence of background materials including Cl^-, SO_4^{2-}, NO_3^-, HCO_3^-, and CO_3^- inhibited DMP degradation in $UV_C/SPS/Fe^{2+}$ system following a trend of $Cl^- < SO_4^{2-} < NO_3^- < HCO_3^- < CO_3^-$.

Dominant radicals during the degradation

In order to determine the role of active species in the DMP degradation process over $UV_C/SPS/Fe^{2+}$, quenching experiments were performed in optimized state. Methanol (MEOH),

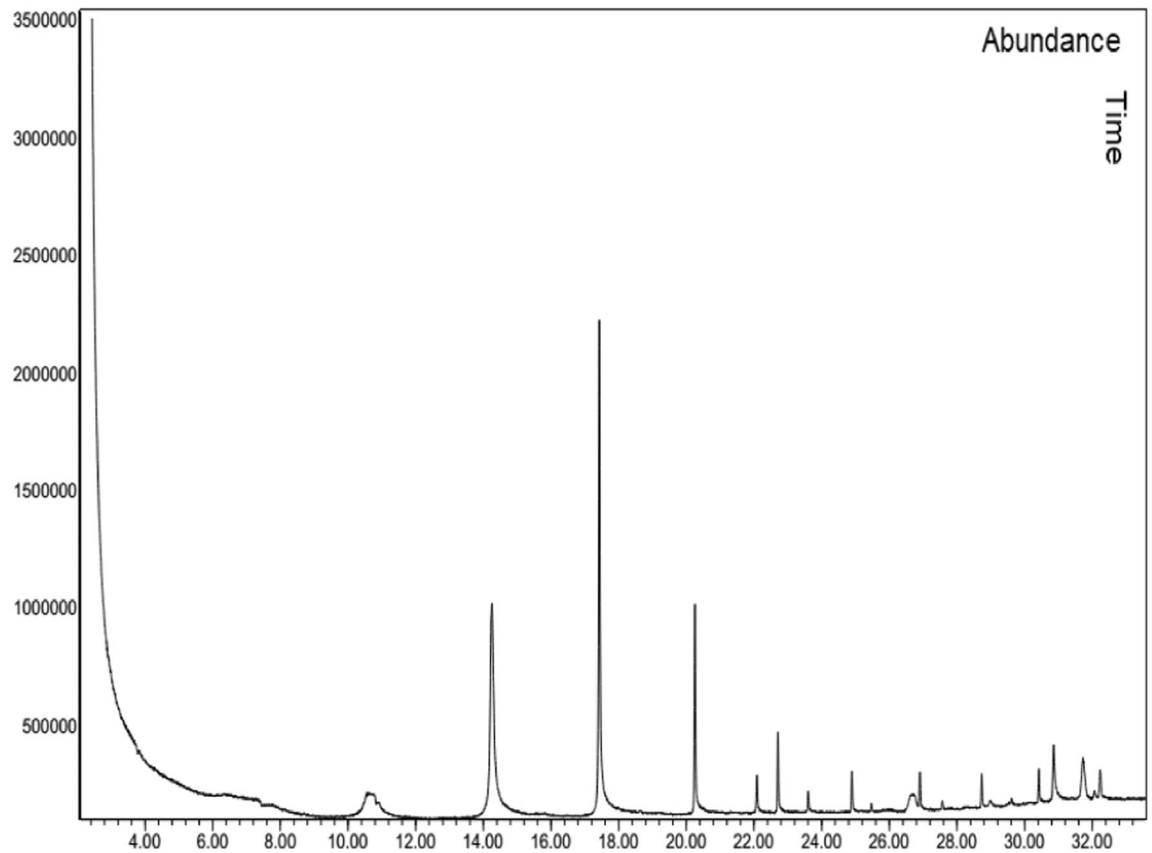

Fig. 6 Gas chromatography of DMP degradation after 90 min

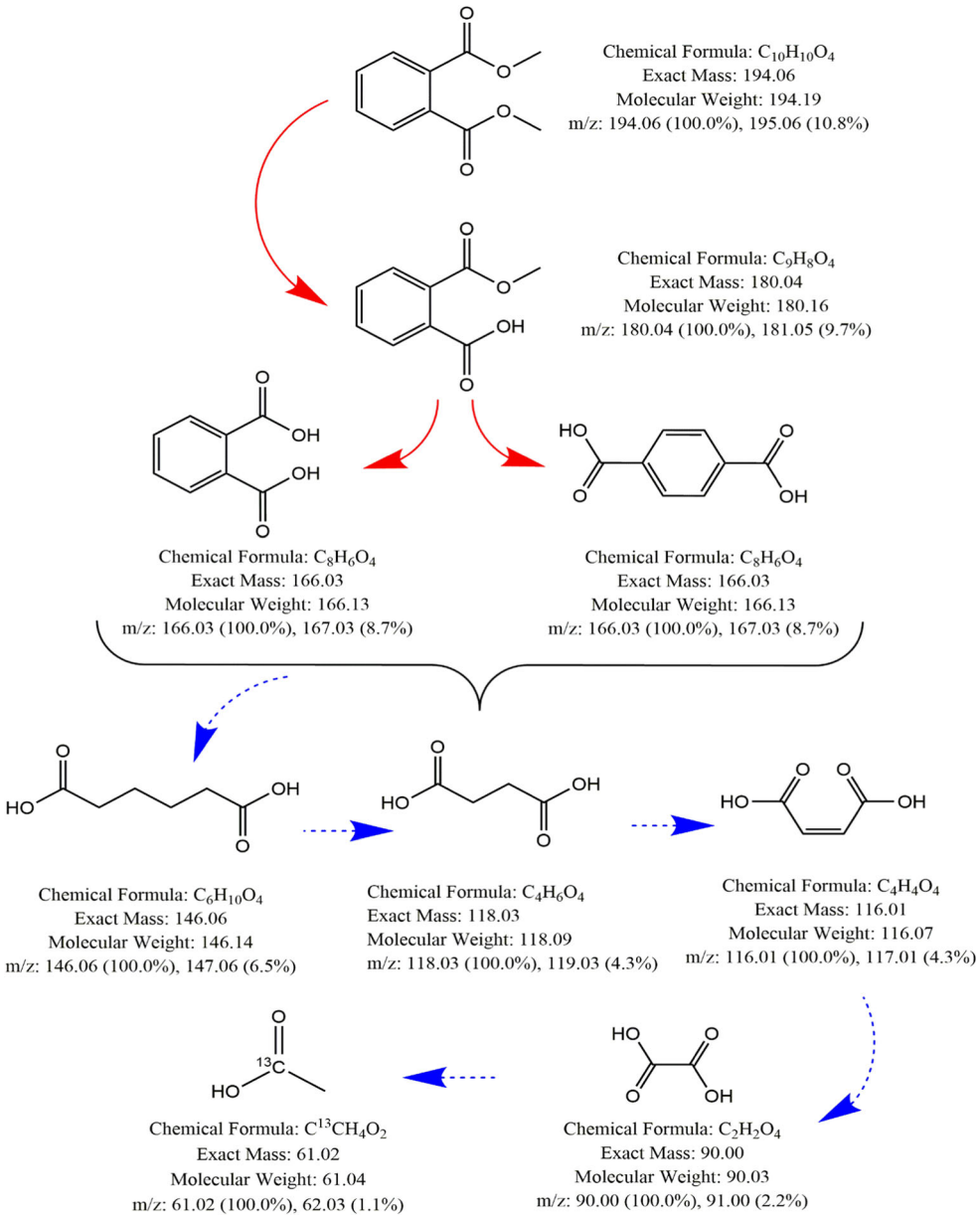

Fig 7 Proposed pathway for degradation of DMP using the $UV_C/SPS/Fe^{2+}$ system

benzoquinone (BQ), potassium iodide (KI) and tert-Butyl alcohol (TBA), all in 500 mM concentration, were used to quench the $SO_4^{\circ-}$, $O_2^{\circ-}$, h^+, and HO° radicals, respectively. The addition of MEOH, BQ and TBA made the DMP degradation decrease to 53%, 70%, and 61%, respectively (Fig. 4a). The above results suggested that the $SO_4^{\circ-}$, $O_2^{\circ-}$, and HO° radicals were involved in the DMP degradation process. Moreover, MEOH and TBA displays stronger inhibiting effect than other one, confirming the SO4°⁻ and HO° as the main active species in degradation process. To further confirm the generation of SO4°⁻ and HO° species, the EPR spectroscopy with 5, 5-dimethyl-1-pyrroline N-oxide (DMPO) as a spin-trapping agent was conducted. As shown in Fig. 4b, the four-line characteristic ESR signal for DMPO-SO4°⁻, a signal for the DMPO-OH° spin adduct were found with characteristic 1:2:2:1 quartet under UV irradiation. ESR results demonstrate that main active species in the UVC/SPS/Fe^{2+} system are the both SO4°⁻ and HO°. However, the spectrum intensity of DMPO-SO4°⁻ was relatively stronger than that of DMPO-OH°. This phenomenon is explained by the fact that DMPO-SO4°⁻ signal diminished quickly over time due to the high reaction rate.

UV–vis and HPLC analysis

The UV absorption spectra variation of DMP during initial and optimized reaction time was shown as Fig. 5a. The UV spectrum of DMP comprises three peak including 195, 280 nm (weak type) and 230 nm (a strong peak). As the reaction progresses until 90 min, the characteristic peaks of

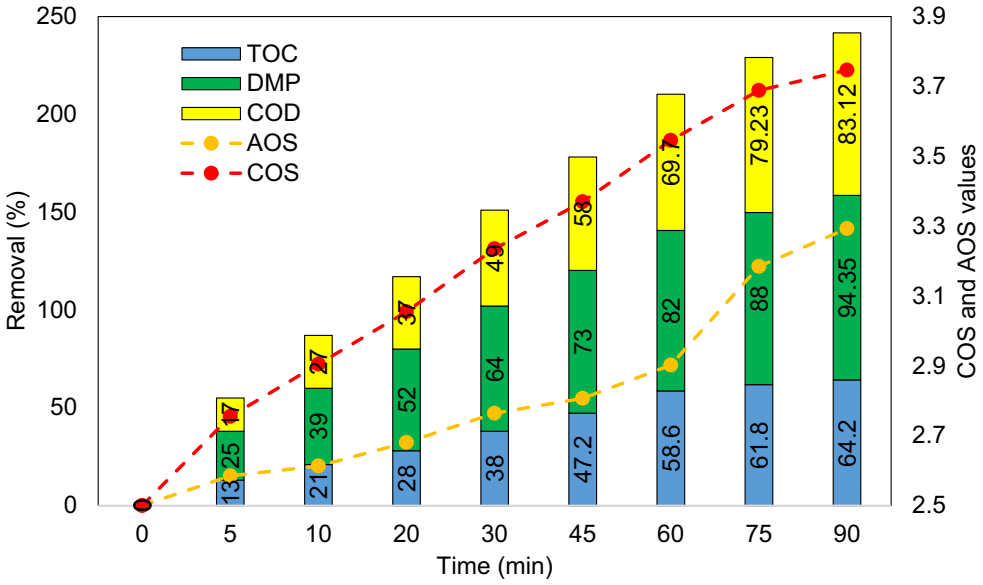

Fig 8 The variation of TOC, COD, AOS and COS parameter during 0 to 90 min degradation time

DMP at 230 and 280 nm disappeared approximately. It emphasizes that the aromatic ring of DMP structure is wrecked and degraded to the straight chain. In other side, the absorption peak of DMP at 195 nm reduced, however did not wholly vanish. It can be due to the one of intermediate products formed in the DMP degradation process that still had an ultraviolet absorption peak in the 195 nm. The chromatographic peak of DMP at 0 and 90 min reaction time (same as UV absorption study) were shown as Fig. 5b. P_1, P_2, P_3 and M chromatographic peak can be observed obviously. The M peak appeared at 2.10 min was attributed to DMP. This maximum peak had downward trend with increasing the degradation time, which indicate that DMP was progressively degraded during the reaction. At the same time, the intermediate product peaks at P_1, P_2 and P_3 generated in the range of 1.28–2.80 min. As can be seen, peaks area of P_1, P_2 and P_3 progressively increased with the time. After optimized time (90 min), M peak reached in its lowest level and the peak area of degradation products was at the highest level. The results confirm the outcomes obtained from UV absorption analysis and indicated that the DMP degradation continued to produce different kinds of intermediates. In the following, GC-MS was used to accurate determination of the intermediates and byproducts derived from the DMP degradation.

GC-MS analysis and proposed degradation pathway

The degradation yields of DMP under UV_C/SPS/Fe^{2+} system at optimized condition were detected by GC-MS. As shown in Fig. 6, during the reaction time (after 90 min), three sharp peaks with retention time of 14.37 min, 17.75 min, and 21.09 min were appeared. The evidence suggests that DMP have been degraded into smaller intermediate products.

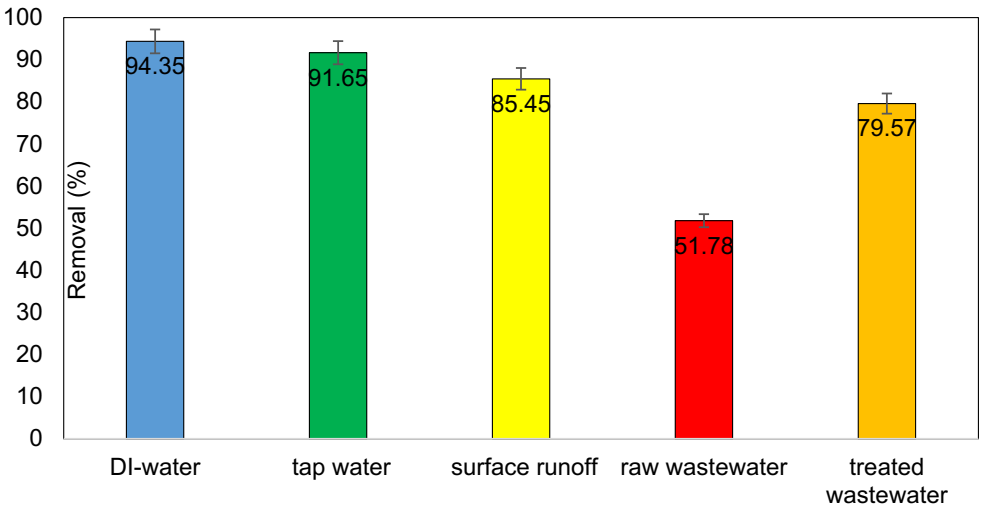

Fig 9 Performance and ability of UV_C/SPS/Fe^{2+} system for DMP degradation in real samples under optimized state

Figure 4S**(a-i)** show the intermediate products of DMP degradation with molecular ion peak in a mass spectrum. From the result of molecular weight and taking into account the HPLC results, it can be concluded that PA, MMP and TPA could be the major intermediates during the degradation of DMP. Moreover, some small molecular organic acid i.e. AA, OA, MA, SA, ADA were resulting products during degradation process. The research result is in agreement with most of previous studies on degradation of DMP [59, 60].

Based on the evidence from UV–vis, HPLC and GC-MS results, the proposed degradation pathways are shown in Fig. 7. Generally, hydrolyzation of the side chain (ester group) of DMP and attacking the predominated oxidizing species i.e. $SO_4^{\circ-}$ and HO° to molecular structure of DMP was found to be the dominant degradation mechanism that occurred in the $UV_C/SPS/Fe^{2+}$ system. The ester group of DMP molecule tend to be directly attacked by free radicals, resulting the side chain ($–COOCH_3$) lost a methoxyl group ($–OCH_3$) and addition of one HO° to formation of the product 1 (MMP). Decarboxylation from MMP via electron transfer from the carboxyl to the $SO_4^{\circ-}$ and step with hydroxylation by one or two HO° radicals led to the formation of isomer 2 (PA) or 3 (TPA). Finally, the aromatic ring of DMP and intermediate products were opened to produce various small molecule organic acids under the attack of $SO_4^{\circ-}$ and HO°. The organic acid (small molecule) are hypothesized to be product 4 (AA), product 5 (OA), product 6 (MA), product 7 (SA), product 8 (ADA), etc. After 90 min of reaction, all the products in the solution were decomposed into carbon dioxide, water and other inorganic salts, achieving the target of complete degradation.

Engineering implications

The mineralization degree of DMP through $UV_C/SPS/Fe^{2+}$ system was measured in term of TOC and COD value variations during the different reaction time under optimum conditions. As shown in Fig. 8, COD and TOC increased to 83.12 and 64.2% after 90 min, and DMP removal rate reached to 94.35%. It can be inferred that the COD and TOC removal efficiency rapidly increases in the initial reaction time and then gradually continue a stable value. This indicates that the intermediates or by-products emerged in the degradation process are highly resistant and are not completely mineralized. In fact, the produced free radicals consumed for degradation of DMP generate by-products which consequently lower simultaneously the mineralization and TOC content. Biodegradability of DMP under studied system were investigated using average oxidation state (AOS) and carbon oxidation state (COS) in optimum circumstances. As shown in Fig. 8, the AOS values before and after degradation process were from 2.5 to 3.29 and COS parameter varied between 2.5 to 3.74 during 90 min reaction, respectively. Improvement these two parameters indicated that $UV_C/SPS/Fe^{2+}$ system can develop the bioavailability of DMP. Hence, applied system can supply promising conditions for biological process.

Performance and ability of $UV_C/SPS/Fe^{2+}$ system in real conditions including tap water, surface runoff, raw wastewater and secondary sedimentation effluent were surveyed. Wastewater characteristics are listed in Table 2S. 5 mg/L DMP was spiked to the samples and experiments were performed in optimum conditions. Degradation efficiencies for tap water, surface runoff, treated and raw wastewater were found to be 91.65, 85.45, 79.57, and 51.78%, respectively, where all percentages are less compared to DI-water (Fig. 9). The reduction can be explained by the fact that quenching free radicals by intervene of high TDS, which makes a competitive mode between various ions and/or organic compound and DMP for adsorption in real condition as well as reactive oxidizing species are two important reasons for reduction in different environments.

Conclusion

The degradation of DMP using a design of experiment (DOE) methodology was studied. The effect of contact time, SPS and Fe^{2+} concentration, pH, and DMP concentration were systematically assessed through the BBD based on RSM approach. Modeling and prediction of the experimental conditions with a high correlation ($R^2 > 0.9984$) successfully was proposed and an optimal experimental levels was also obtained via desirability function (DF > 0.97221). The high agreement between the results of process optimization (97.227% removal efficiency) and its repetition in real terms (94.35%) confirmed the applicability of RSM-BBD model for optimization of DMP degradation using $UV_C/SPS/Fe^{2+}$ system. The scavenging experiments showed that hydroxyl and sulfate radicals play an important role in the degradation process, in which sulfate radicals is more predominant. The results showed that the background materials could have a negative effect on the removal efficiency as $Cl^- < SO_4^{2-} < NO_3^- < HCO_3^- < CO_3^-$. The intermediates products derived from DMP degradation were determined by HPLC and GC-MS analysis and reaction pathway were proposed.

Acknowledgments This work was supported by: Iran University of Medical Sciences. The authors would like to gratefully appreciate Iran University of Medical Sciences for financial supports (Grant No. 2566).

Compliance with ethical standards

Conflict of interest All authors have no conflict of interest to declare.

References

1. Esplugas S, Bila DM, Krause LGT, Dezotti M. Ozonation and advanced oxidation technologies to remove endocrine disrupting chemicals (EDCs) and pharmaceuticals and personal care products (PPCPs) in water effluents. J Hazard Mater. 2007;149(3):631–42.
2. Safari GH, Nasseri S, Mahvi AH, Yaghmaeian K, Nabizadeh R, Alimohammadi M. Optimization of sonochemical degradation of tetracycline in aqueous solution using sono-activated persulfate process. J Environmental Health Science Engineering. 2015;13(1):76.
3. Ahmadi E, Gholami M, Farzadkia M, Nabizadeh R, Azari A. Study of moving bed biofilm reactor in diethyl phthalate and diallyl phthalate removal from synthetic wastewater. Bioresour Technol. 2015;183:129–35.
4. Yegane badi M, Fallah Jokandan S, Esrafili A, Ahmadi E, Azari A, Mokhtari S, et al. Efficacy of advanced oxidation process persulfate-based (UV / Na2S2O8 / Fe2+) for phthalic acid removal from aqueous solutions. J Babol University Medical Sciences. 2018;20(2):0.
5. Roslev P, Vorkamp K, Aarup J, Frederiksen K, Nielsen PH. Degradation of phthalate esters in an activated sludge wastewater treatment plant. Water Res. 2007;41(5):969–76.
6. Oliver R, May E, Williams J. Microcosm investigations of phthalate behaviour in sewage treatment biofilms. Sci Total Environ. 2007;372(2–3):605–14.
7. Deblonde T, Cossu-Leguille C, Hartemann P. Emerging pollutants in wastewater: a review of the literature. Int J Hyg Environ Health. 2011;214(6):442–8.
8. Sun K, Jin J, Keiluweit M, Kleber M, Wang Z, Pan Z, et al. Polar and aliphatic domains regulate sorption of phthalic acid esters (PAEs) to biochars. Bioresour Technol. 2012;118:120–7.
9. Fang C-R, Yao J, Zheng Y-G, Jiang C-J, Hu L-F, Wu Y-Y, et al. Dibutyl phthalate degradation by Enterobacter sp. T5 isolated from municipal solid waste in landfill bioreactor. Int Biodeterior Biodegradation. 2010;64(6):442–6.
10. Liao C-S, Chen L-C, Chen B-S, Lin S-H. Bioremediation of endocrine disruptor di-n-butyl phthalate ester by Deinococcus radiodurans and pseudomonas stutzeri. Chemosphere. 2010;78(3):342–6.
11. Psillakis E, Mantzavinos D, Kalogerakis N. Monitoring the sonochemical degradation of phthalate esters in water using solid-phase microextraction. Chemosphere. 2004;54(7):849–57.
12. Cases V, Alonso V, Argandoña V, Rodriguez M, Prats D. Endocrine disrupting compounds: a comparison of removal between conventional activated sludge and membrane bioreactors. Desalination. 2011;272(1–3):240–5.
13. Ahel M, Mikac N, Cosovic B, Prohic E, Soukup V. The impact of contamination from a municipal solid waste landfill (Zagreb, Croatia) on underlying soil. Water Sci Technol. 1998;37(8):203–10.
14. Chu W, Li D, Gao N, Templeton MR, Tan C, Gao Y. The control of emerging haloacetamide DBP precursors with UV/persulfate treatment. Water Res. 2015;72:340–8.
15. Mazloomi S, Nasseri S, Nabizadeh R, Yaghmaeian K, Alimohammadi K, Nazmara S, et al. Remediation of fuel oil contaminated soils by activated persulfate in the presence of MnO2. Soil and Water Research. 2016;11(2):131–8.
16. Hazime R, Nguyen Q, Ferronato C, Salvador A, Jaber F, Chovelon J-M. Comparative study of imazalil degradation in three systems: UV/TiO2, UV/K2S2O8 and UV/TiO2/K2S2O8. Appl Catal B Environ. 2014;144:286–91.
17. Huang K-C, Zhao Z, Hoag GE, Dahmani A, Block PA. Degradation of volatile organic compounds with thermally activated persulfate oxidation. Chemosphere. 2005;61(4):551–60.
18. Dehghani S, Jafari AJ, Farzadkia M, Gholami M. Sulfonamide antibiotic reduction in aquatic environment by application of Fenton oxidation process. Iranian J Environmental Health Sci Engineering. 2013;10(1):29.
19. Mokhtari SA, Farzadkia M, Esrafili A, Kalantari RR, Jafari AJ, Kermani M, et al. Bisphenol a removal from aqueous solutions using novel UV/persulfate/H 2 O 2/cu system: optimization and modelling with central composite design and response surface methodology. J Environ Health Sci Eng. 2016;14(1):19.
20. Silveira JE, Paz WS, Garcia-Munoz P, Zazo JA, Casas JA. UV-LED/ilmenite/persulfate for azo dye mineralization: the role of sulfate in the catalyst deactivation. Appl Catal B Environ. 2017;219:314–21.
21. Shih Y-J, Putra WN, Huang Y-H, Tsai J-C. Mineralization and deflourization of 2, 2, 3, 3-tetrafluoro-1-propanol (TFP) by UV/persulfate oxidation and sequential adsorption. Chemosphere. 2012;89(10):1262–6.
22. Mohammadi F, Alimohammadi M, Mahvi A, Nazmara S, Mazloomi S, Aslani H. Removal of TPHs from soil media using persulfate oxidant in the presence of mineral siderite. Malaysian J Soil Sci. 2016;20:67–78.
23. Ghaneian MT, Tabatabaee M, Ehrampush MH, Nafisi M, Amrollahi M, Taghavi M. Survey of photochemical oxidation efficiency of 2, 4-dichlorophenoxyacetic acid using s_2o_8/uv from aqueous solution. 2017.
24. Zhao L, Hou H, Fujii A, Hosomi M, Li F. Degradation of 1, 4-dioxane in water with heat-and Fe 2+−activated persulfate oxidation. Environ Sci Pollut Res. 2014;21(12):7457–65.
25. De Luca A, He X, Dionysiou DD, Dantas RF, Esplugas S. Effects of bromide on the degradation of organic contaminants with UV and Fe2+ activated persulfate. Chem Eng J. 2017;318:206–13.
26. Rao Y, Xue D, Pan H, Feng J, Li Y. Degradation of ibuprofen by a synergistic UV/Fe (III)/Oxone process. Chem Eng J. 2016;283:65–75.
27. Yegane badi M, Azari A, Esrafili A, Ahmadi E, Gholami M. Performance evaluation of magnetized multiwall carbon nanotubes by iron oxide nanoparticles in removing fluoride from aqueous solution. J Mazandaran University Medical Sci. 2015;25(124):128–42.
28. Badi MY, Azari A, Pasalari H, Esrafili A, Farzadkia M. Modification of activated carbon with magnetic Fe 3 O 4 nanoparticle composite for removal of ceftriaxone from aquatic solutions. J Mol Liq 2018.
29. Azari A, Gholami M, Torkshavand Z, Yari A, Ahmadi E, Kakavandi B. Evaluation of basic violet 16 adsorption from aqueous solution by magnetic zero valent iron-activated carbon nanocomposite using response surface method: isotherm and kinetic studies. J Mazandaran University Medical Sci. 2015;24(121):333–47.
30. Azari A, Esrafili A, Ahmadi E, Gholami M. Performance evaluation of magnetized multiwall carbon nanotubes by iron oxide nanoparticles in removing fluoride from aqueous solution. J Mazandaran University Medical Sci. 2015;25(124):128–42.
31. Kalantary RR, Azari A, Esrafili A, Yaghmaeian K, Moradi M, Sharafi K. The survey of malathion removal using magnetic graphene oxide nanocomposite as a novel adsorbent: thermodynamics, isotherms, and kinetic study. Desalin Water Treat. 2016;57(58):28460–73.
32. Gorji ME, Ahmadkhaniha R, Moazzen M, Yunesian M, Azari A, Rastkari N. Polycyclic aromatic hydrocarbons in Iranian kebabs. Food Control. 2016;60:57–63.
33. Lin K-YA, Zhang Z-Y. Degradation of bisphenol a using peroxymonosulfate activated by one-step prepared sulfur-doped carbon nitride as a metal-free heterogeneous catalyst. Chem Eng J. 2017;313:1320–7.

34. Jorfi S, Kakavandi B, Motlagh HR, Ahmadi M, Jaafarzadeh N. A novel combination of oxidative degradation for benzotriazole removal using TiO2 loaded on FeIIFe2IIIO4@ C as an efficient activator of peroxymonosulfate. Appl Catal B Environ. 2017;219:216–30.
35. Mirzaei N, Ghaffari HR, Sharafi K, Velayati A, Hoseindoost G, Rezaei S, et al. Modified natural zeolite using ammonium quaternary based material for acid red 18 removal from aqueous solution. J Environmental Chem Engineering. 2017;5(4):3151–60.
36. Rastogi A, Al-Abed SR, Dionysiou DD. Sulfate radical-based ferrous–peroxymonosulfate oxidative system for PCBs degradation in aqueous and sediment systems. Appl Catal B Environ. 2009;85(3–4):171–9.
37. Antoniou MG, Boraei I, Solakidou M, Deligiannakis Y, Abhishek M, Lawton LA, et al. Enhancing photocatalytic degradation of the cyanotoxin microcystin-LR with the addition of sulfate-radical generating oxidants. J Hazard Mater. 2018;360:461–70.
38. Cheng M, Zeng G, Huang D, Lai C, Xu P, Zhang C, et al. Hydroxyl radicals based advanced oxidation processes (AOPs) for remediation of soils contaminated with organic compounds: a review. Chem Eng J. 2016;284:582–98.
39. Ai Z, Yang P, Lu X. Degradation of 4-chlorophenol by a microwave assisted photocatalysis method. J Hazard Mater. 2005;124(1–3):147–52.
40. An T, Gao Y, Li G, Kamat PV, Peller J, Joyce MV. Kinetics and mechanism of •OH mediated degradation of dimethyl phthalate in aqueous solution: experimental and theoretical studies. Environ Sci Technol. 2014;48(1):641–8.
41. Yegane badi M, Esrafili A, Rezaei Kalantary R, Azari A, Ahmadi E, Gholami M. Removal of diethyl phthalate from aqueous solution using persulfate-based (UV/Na2S2O8/Fe2+) advanced oxidation process. J Mazandaran University Medical Sci. 2016;25(132):122–35.
42. Lin H, Wu J, Zhang H. Degradation of bisphenol a in aqueous solution by a novel electro/Fe3+/peroxydisulfate process. Sep Purif Technol. 2013;117:18–23.
43. Rezaei Kalantary R, Dehghanifard E, Mohseni-Bandpi A, Rezaei L, Esrafili A, Kakavandi B, et al. Nitrate adsorption by synthetic activated carbon magnetic nanoparticles: kinetics, isotherms and thermodynamic studies. Desalin Water Treat. 2016;57(35):16445–55.
44. Azadbakht F, Esrafili A, Yeganeh Badi M, Sajedifar J, Amiri M, Gholami M. Efficiency of persulfate-based advanced oxidation process (UV/Na2S2O8) in removal of metronidazole from aqueous solutions. J Mazandaran University Med Sci. 2017;27(154):119–29.
45. Sun DD, Yan XX, Xue WP, editors. Oxidative degradation of dimethyl phthalate (DMP) by persulfate catalyzed by Ag+ combined with microwave irradiation. Advanced Materials Research; 2013: Trans Tech Publ.
46. Shiying Y, Ping W, Xin Y, Guang W, Zhang W, Liang S. A novel advanced oxidation process to degrade organic pollutants in wastewater: microwave-activated persulfate oxidation. J Environ Sci. 2009;21(9):1175–80.
47. Peyton GR. The free-radical chemistry of persulfate-based total organic carbon analyzers. Mar Chem. 1993;41(1–3):91–103.
48. Chu W, Wang Y, Leung H. Synergy of sulfate and hydroxyl radicals in UV/S2O82−/H2O2 oxidation of iodinated X-ray contrast medium iopromide. Chem Eng J. 2011;178:154–60.
49. Guo Y, Zhou J, Lou X, Liu R, Xiao D, Fang C, et al. Enhanced degradation of Tetrabromobisphenol a in water by a UV/base/persulfate system: kinetics and intermediates. Chem Eng J. 2014;254:538–44.
50. Huang Y-F, Huang Y-H. Identification of produced powerful radicals involved in the mineralization of bisphenol a using a novel UV-Na2S2O8/H2O2-Fe (II, III) two-stage oxidation process. J Hazard Mater. 2009;162(2–3):1211–6.
51. Wu J, Zhang H, Qiu J. Degradation of acid Orange 7 in aqueous solution by a novel electro/Fe2+/peroxydisulfate process. J Hazard Mater. 2012;215:138–45.
52. Liu C, Shih K, Sun C, Wang F. Oxidative degradation of propachlor by ferrous and copper ion activated persulfate. Sci Total Environ. 2012;416:507–12.
53. Du ED, Feng XX, Guo YQ, Peng MG, Feng HQ, Wang JL, et al. Dimethyl phthalate degradation by UV/H2O2: combination of experimental methods and quantum chemical calculation. CLEAN–Soil, Air, Water. 2015;43(6):811–21.
54. Azari A, Kakavandi B, Kalantary RR, Ahmadi E, Gholami M, Torkshavand Z, et al. Rapid and efficient magnetically removal of heavy metals by magnetite-activated carbon composite: a statistical design approach. J Porous Mater. 2015;22(4):1083–96.
55. Kakavandi B, Jahangiri-rad M, Rafiee M, Esfahani AR, Babaei AA. Development of response surface methodology for optimization of phenol and p-chlorophenol adsorption on magnetic recoverable carbon. Microporous Mesoporous Mater. 2016;231:192–206.
56. Jafari AJ, Kakavandi B, Kalantary RR, Gharibi H, Asadi A, Azari A, et al. Application of mesoporous magnetic carbon composite for reactive dyes removal: process optimization using response surface methodology. Korean J Chem Eng. 2016;33(10):2878–90.
57. Ma J, Yang Y, Jiang X, Xie Z, Li X, Chen C, et al. Impacts of inorganic anions and natural organic matter on thermally activated persulfate oxidation of BTEX in water. Chemosphere. 2018;190:296–306.
58. Neta P, Huie RE, Ross AB. Rate constants for reactions of inorganic radicals in aqueous solution. J Phys Chem Ref Data. 1988;17(3):1027–284.
59. B-l Y, Li X-z, Graham N. Reaction pathways of dimethyl phthalate degradation in TiO2–UV–O2 and TiO2–UV–Fe (VI) systems. Chemosphere. 2008;72(2):197–204.
60. Wu M-H, Liu N, Xu G, Ma J, Tang L, Wang L, et al. Kinetics and mechanisms studies on dimethyl phthalate degradation in aqueous solutions by pulse radiolysis and electron beam radiolysis. Radiat Phys Chem. 2011;80(3):420–5.